

Tensile strength prediction of corroded steel plates by using machine learning approach

Cindy N.N. Karina^a, Pang-jo Chun^{*}, and Kazuaki Okubo^b

Department of Civil and Environmental Engineering, Ehime University, 3 Bunkyo-cho, Matsuyama, Ehime 790-8577, Japan

(Received May 30, 2016, Revised May 15, 2017, Accepted May 17, 2017)

Abstract. Safety service improvement and development of efficient maintenance strategies for corroded steel structures are undeniably essential. Therefore, understanding the influence of damage caused by corrosion on the remaining load-carrying capacities such as tensile strength is required. In this study, artificial neural network (ANN) approach is proposed in order to produce a simple, accurate, and inexpensive method developed by using tensile test results, material properties and finite element method (FEM) results to train the ANN model. Initially in reproducing corroded model process, FEM was used to obtain tensile strength of artificial corroded plates, for which surface is developed by a spatial autocorrelation model. By using the corroded surface data and material properties as input data, with tensile strength as the output data, the ANN model could be trained. The accuracy of the ANN result was then verified by using leave-one-out cross-validation (LOOCV). As a result, it was confirmed that the accuracy of the ANN approach and the final output equation was developed for predicting tensile strength without tensile test results and FEM in further work. Though previous studies have been conducted, the accuracy results are still lower than the proposed ANN approach. Hence, the proposed ANN model now enables us to have a simple, rapid, and inexpensive method to predict residual tensile strength more accurately due to corrosion in steel structures.

Keywords: corrosion; tensile test; finite element analysis; artificial neural network

1. Introduction

Many steel bridge infrastructures in the world are getting older, and large number of these structures is in need of maintenance, rehabilitation or replacement. Most of them are subjected to corrosion due to the exposure to aggressive environmental conditions and inadequate maintenance (Kaita *et al.* 2012). Corrosion has a harmful consequence from the safety point of view and can lead to thickness penetration, fatigue cracks, brittle fracture and unstable failure (Khedmati *et al.* 2011). Evaluation of existing steel structures due to deterioration caused by corrosion, natural aging, increasing load spectra, increasing seismic demand, and other problems becomes vital (Ohga *et al.* 2011). Therefore, understanding the influence of damage on the remaining load-carrying capacities is required.

Previously, several experimental studies and detailed investigations of corroded surface have been carried out by other researchers (Muranaka *et al.* 1998, Rahgozar *et al.* 2010) and our research group (Appuhamy *et al.* 2011, 2013), to evaluate new methods of estimating the residual strength capacities of corroded steel plates. Since the corroded surface differs from each other so does the complexity of their irregularities, previous experimental studies, and analytical studies fail to give highly accurate

results as it is produced in this proposed method, artificial neural network (ANN), which is expected to be a simple, rapid, and inexpensive approach to predict tensile strength more accurately.

The application of ANN in the field of pharmaceutical development and optimization of dosage forms has recently gained interest (Hussain *et al.* 1991, 1994, Murtoniemi *et al.* 1993, Richardson and Barlow 1996, Bozic 1996). In some of these papers the ANN modelling methodology successfully produced better results compared to other classical statistical learning methods. Thus, in this study, ANN is adopted within the scope of steel structures in order to obtain an accurate assessment method. The accuracy of the proposed method was then verified by the leave-one-out cross validation (LOOCV) method.

2. Verification of validity of Finite Element Method (FEM) by a tensile experiment on corroded steel plates

2.1 Corroded plate thickness measurement

The test specimens were cut out from steel girders of Ananai River Bridge in Kochi Prefecture and Funakoshi Bridge in Ehime Prefecture in Japan. There were 30 corroded steel specimens in total: 18 from Ananai Bridge, and 12 from Funakoshi Bridge. The specimens were named as ANT-1 to ANT-18, FUT-1 to FUT-12, corresponding to Ananai Bridge and Funakoshi Bridge respectively. The first two letters of the coding name rule are taken from the first two letters of the bridge name and the last letter T is taken

*Corresponding author, Ph.D., Associate Professor,

E-mail: chun@cee.ehime-u.ac.jp

^a Ph.D. Student

^b Associate Professor

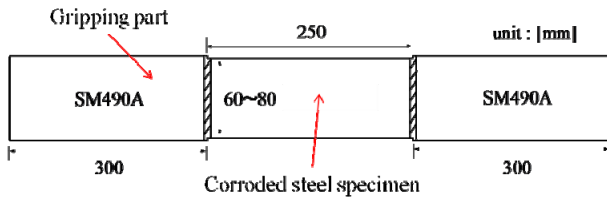
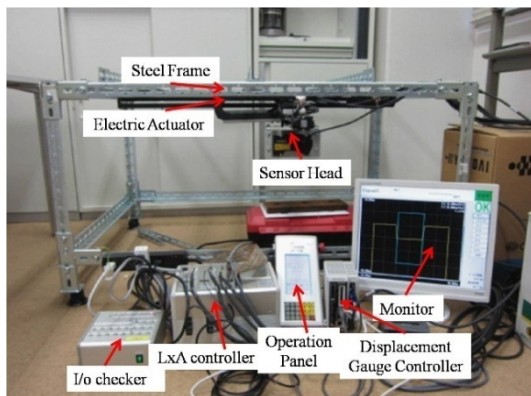


Fig. 1 Corroded test specimens

Table 1 Material properties

Specimens	Modulus of elasticity (GPa)	Poisson's ratio	Yield stress (MPa)	Tensile strength (MPa)	Fracture elongation (%)
Ananai Bridge	197.4	0.272	281.6	431.3	40.2
Funakoshi Bridge	208	0.280	280.0	437.6	40.6



(a) 3D laser measuring device



(b) Thickness measurement by 3D measuring device

Fig. 2 Measuring device and thickness measurement by 3D measuring device

from the first letter of 'Tensile test'.

Before conducting the thickness measurement, all the rust over both surfaces was removed carefully by using electric wire brushes and punches. This step was then followed by welding the gripping part to corroded steel specimen. The center line of gripping part and specimen

were aligned carefully using laser line marker in order to prevent angular distortion. The gripping parts, new SM490A plates, were jointed to both end surface sides of the specimen by butt full penetration welding, as shown in Fig. 1. In addition, six corrosion-free-specimens (JIS5 type) were made, three each from the Ananai Bridge and Bridge, and tensile tests were carried out to clarify the material properties of the test specimens. The material properties obtained from these tests are shown in Table 1. Since accuracy and convenience are highly demanded in the measurement of corroded surface irregularities, a portable three-dimensional (3D) scanning system was used in this surface measurement, as shown in Fig. 2(a). The 3D measuring device allows us to measure 3D coordinate values at any arbitrary point on a corroded surface directly and continuously (Kaita *et al.* 2005). The device can measure the coordinates of a point on a steel surface by using a non-contact scanning probe (laser line probe). Measurement of the corroded thickness is shown in Fig. 2(b). Since this probe scans the steel surface with a laser beam, which is about 100 mm wide, a large amount of 3D coordinate data can be obtained quickly. With this measuring device, the 3D coordinate data are obtained as numerous in-line dots; the accuracy of the device is about 0.1 mm. The thicknesses of all scratched specimens were measured by using this 3D laser scanning device, and the coordinate data were collected in a grid of 0.5mm intervals in both the x - and y - directions. From that measurement process, the average thickness and minimum thickness could be obtained for each interval. The minimum average thickness was calculated by taking the minimum value from all average thicknesses in each interval. The remaining statistical thickness parameters, such as the standard deviation of thickness were then also calculated from those thickness measurement results.

2.2 Tensile test of corroded steel specimens

Tensile tests were carried out under loading control at a constant velocity by using a hydraulic loading test machine (maximum load: 2940 kN) for all 30 specimens, with different levels of corrosion. The loading velocity was set to 150 N/s to avoid dynamic failure. One of the prepared specimens with previously attached strain gauges on it can be seen in Fig. 3.



Fig. 3 Specimen prepared for tensile test

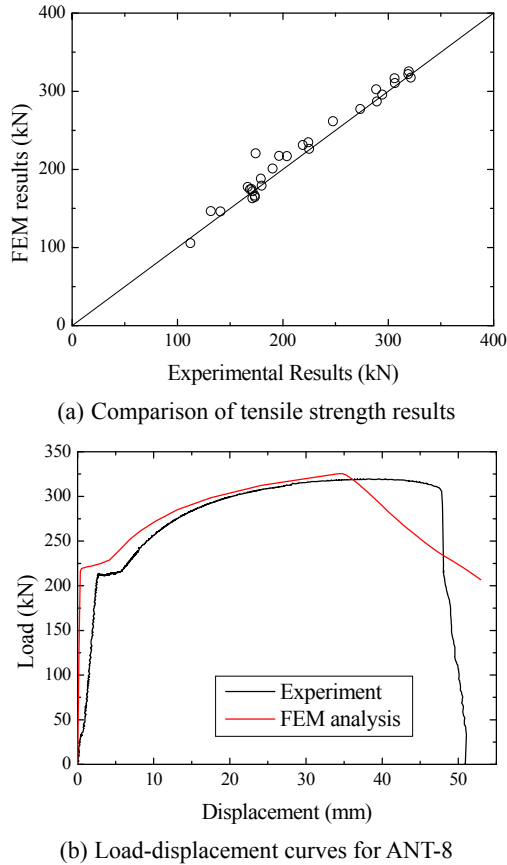


Fig. 4 Comparison results between FEM results and experimental results

2.3 Verification of the validity of FEM

Previously, another study on mechanical behavior of heat-corrected steel plates (Chun and Inoue 2009) had FEM model verification done with their experimental results. It was found that their FEM model was well validated. Likewise, in this study, FEM was examined by comparing them to the tensile test results, as shown in Fig. 4. Finite element analysis (FEA) has been used to reproduce many corroded surface shapes by using a spatial autocorrelation model in order to train the ANN model.

As seen in Fig. 4(a), tensile strength values between FEM and experiment were almost equivalent and comparison results for specimen ANT-8 can be seen in Fig. 4(b) which shows that the maximum load is quite similar between the FEM results and the experimental results. The load-displacement curve in Fig. 4(b) also indicates that the comparison results gave a very good agreement. Though there is discrepancy due to the slipping at the gripping part which was observed at the initial stage of experiment, these comparison results indicate that the FEM model is well validated, and the FEM model can be used for developing ANN model.

3. Structure of training data set

In order to train an ANN model, input data such as corroded surface data and material properties are required,

as well as tensile strength as output data. Since the objective of this study is to find accurate results, it is vital to have large set of data. Therefore, in this study, a commercial software package Abaqus/standard was used to perform the FEM analysis. Thereby, many corroded surface shapes can be artificially produced by the spatial autocorrelation model proposed by Okumura *et al.* (2001) which can be used for developing an FEM model. A spatial autocorrelation model was made by taking into account the correlation between the corrosion depths of each node on the corrosion surface. By Eq. (1), the corrosion depth distribution was derived, where V_i' is the corrosion depth at the i -th measurement point, V_i is the independent corrosion depth at the i -th measurement point, β is the distance attenuation coefficient, and d_{ij} is the distance between point i and point j .

$$\begin{pmatrix} V_1' \\ V_2' \\ \vdots \\ V_n' \end{pmatrix} = \begin{pmatrix} 1 & e^{-\beta d_{21}} & \dots & e^{-\beta d_{n1}} \\ e^{-\beta d_{12}} & 1 & \dots & e^{-\beta d_{n2}} \\ \vdots & \vdots & \ddots & \vdots \\ e^{-\beta d_{1n}} & e^{-\beta d_{2n}} & \dots & e^{-\beta d_{nn}} \end{pmatrix} \begin{pmatrix} V_1 \\ V_2 \\ \vdots \\ V_n \end{pmatrix} \quad (1)$$

By referring to Okumura *et al.* (2001) β values are between 0.28 to 0.4 and in this study β values were set randomly between those values. As for independent corrosion depth values V_i , a random number generated from Poisson distribution was used by referring to Okumura *et al.* (2001). As for the parameter range shown in Table 2 of average thickness, minimum average thickness, minimum thickness, standard deviation, Young's modulus, yield strength and ultimate strength were set by referring to the experimental results and measurement data. As for the range of initial plate thicknesses, width, and length were set by using truncated random variables.

By using all these aforementioned parameters, 1000 plates were successfully generated in this study. Furthermore, 3D 8-node hexadral elements (C3D8) were used in the FEM model to represent the complexity of actual corroded steel specimens. Ahmmad and Sumi (2010) previously investigated the deformability of corroded steel plates under quasistatic uniaxial tension caused by pitting corrosion and general corrosion. In this study, a pitting corrosion case was also generated by creating oval-shaped

Table 2 Parameters taken from measurement and experimental results

Parameter	Range
Initial thickness [mm]	10.0~40.0
Width [mm]	20.0~150.0
Length [mm]	202.0~1500.0
Average thickness [mm]	4.6~36.6
Minimum average thickness [mm]	1.6~33.5
Minimum thickness [mm]	0.003~27.9
Standard deviation [mm]	0.172~5.307
Young's modulus [GPa]	180.0~219.8
Yield strength [MPa]	200.0~290.0
Ultimate strength [MPa]	390.0~520.0

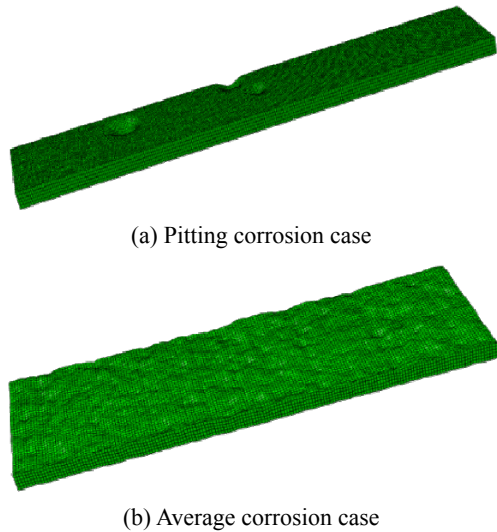


Fig. 5 Artificial corroded models reproduced by spatial autocorrelation model

corrosion and general corrosion case on the plate surface randomly using autocorrelation model as shown in Fig. 5. A 2-mm regular mesh pattern was adopted for all the analytical models. One edge of the member's translation in the x -, y -, and z - directions was fixed and only the y -, and z -direction translations of the other edge (loading edge) were fixed, to simulate the actual experimental conditions. Uniform incremental displacement was then applied to the loading edge. FEA validation was confirmed as mentioned in the previous section.

4. Framework of artificial neural network

4.1 Overview of artificial neural network

The tensile strength prediction method has been developed by using a multilayer perceptron feed-forward artificial neural network as depicted in Fig. 6. ANN consists of multiple layers including an input layer, hidden layer(s), and an output layer. These layers have nodes interconnected with the nodes of adjoining layers by synapses. Figure 5 in the Fig. 6 is the activation function which is chosen as the sigmoidal function as formulated in Eq. (2).

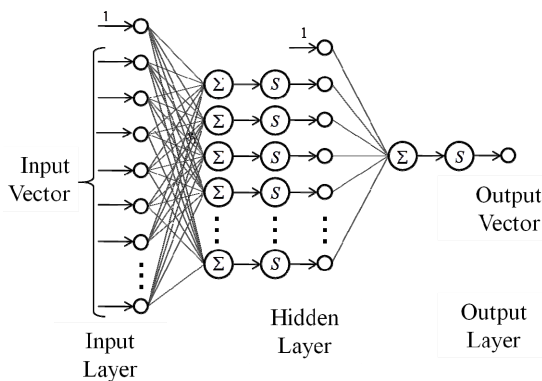


Fig. 6 Typical feed-forward artificial neural network

$$S(a) = \frac{2}{1 + \exp(-2a)} - 1 \quad (2)$$

where a is the input of the activation function. Oriented synapses which connect the nodes and the strength of a connection between two nodes are respectively called synaptic neurons and synaptic weight. The synaptic weight is updated in order to increase the accuracy of neural network by minimizing the sum-squared error norm $E(\mathbf{w})$ as shown in Eq. (3).

$$E(\mathbf{w}) = \frac{1}{2} \sum_{n=1}^N \|\mathbf{y}(\mathbf{x}_n, \mathbf{w}) - \mathbf{t}_n\|^2 \quad (3)$$

\mathbf{w} is the synaptic weight vector, \mathbf{x}_n is a set of input vectors, $\mathbf{y}(\mathbf{x}_n, \mathbf{w})$ is the vector of output variables, \mathbf{t}_n is a corresponding set of target vectors, N is the number of data set (input-output). Though the Back-propagation algorithm is a well-known algorithm to minimize $E(\mathbf{w})$ in Eq. (3), the formula still lacks computation speed. Therefore, in this study, the Levenberg-Marquardt optimization algorithm has been used because it performed better than other algorithms in terms of convergence rate (El-Bakyr 2003). In the Levenberg-Marquardt algorithm, the weight vector can be adjusted iteratively as given in Eq. (4).

$$\mathbf{w}^{(r+1)} = \mathbf{w}^{(r)} - [\mathbf{J}^T \mathbf{J} + \mu \mathbf{I}]^{-1} \mathbf{J}^T \mathbf{e} \quad (4)$$

\mathbf{e} is the error vector, \mathbf{J} is the Jacobian matrix which contains the first derivatives of the error \mathbf{e} in the network by means at weights \mathbf{w} and bias, \mathbf{I} is the identity matrix, r is the number of iterations, μ is the Marquardt parameter, and in this study, 0.001 was used as an initial value.

The number of nodes in input layer is the amount of input data; there are ten nodes in this study. The nodes represent initial thickness, plate width, plate length, Young's modulus, yield strength, ultimate strength, average thickness, minimum average thickness, standard deviation of thickness, and minimum thickness. On the other hand, the output value in this ANN system is only tensile strength, thus the number of nodes in output layer is one. In order to obtain positive values in the ANN system, instead of using the tensile strength result directly as output data, a log logarithm of tensile strength was applied in this study. As for hidden layer(s), the number of nodes was obtained by doing trial and error to achieve an optimal number, and was set to eight. Furthermore, the bagging method is known as an effective way to achieve high accuracy by taking the average value from each output in order that a new and more accurate output result can be obtained (Hastie *et al.* 2014). Since it is desirable to improve the accuracy of the output result, the bagging method was applied in this study. Here, specifically in this study, ten generated neural network models were evaluated by the bagging method and the average output value was then used as the final result, which was more accurate than the previous output. The number of neural network models literally influences the accuracy of the result, and yet there is still no numerical method to determine the optimum number of the ANN model. Therefore, by trial and error, it was found that, with

ten generated values, the accuracy was already converged.

4.2 Accuracy verification

Verification of the validity of the neural network model generated in the previous section will be performed by LOOCV method in this section. LOOCV is a validation method that will train all the data except for one datum and the prediction will be made for that one datum (Bishop 2007). This process was repeated until the rest of the overall data set had been trained. As discussed previously, in this study, 1000 data set (input-output) was prepared. ANN was trained primarily by using only 999 data due to the one datum was taken out from the data set to be analyzed. This process was repeated 1000 times until all data sets had been evaluated in order to verify the accuracy of ANN results. Moreover, the mean absolute error percentage was also derived by using the following Eq. (5) to evaluate the performance quantitatively. In the equation below, N is the number of data set (input-output), y_t is the target data, and y_p is the predicted result.

$$\text{Mean absolute error percentage} = \frac{1}{N} \sum_{i=1}^N \left| \frac{y_t - y_p}{y_t} \right| \quad (5)$$

In this study, it is necessary to investigate the relationship of all ten parameters mentioned in the previous section to analyze the result by considering five different cases as

shown in the following list, and the validation results can be seen in Figs. 7 to 11 for cases 1 to 5 respectively. Experiment shows that the accuracy increases with the number of parameter which is because the ANN is stronger against the multicollinearity than other statistical method (Zhang 2003). The error percentages derived from Eq. (5) are summarized in Table 3.

- (1) All parameters were included
- (2) Average thickness, plate width, plate length, initial thickness, young modulus, ultimate strength, yield strength were included

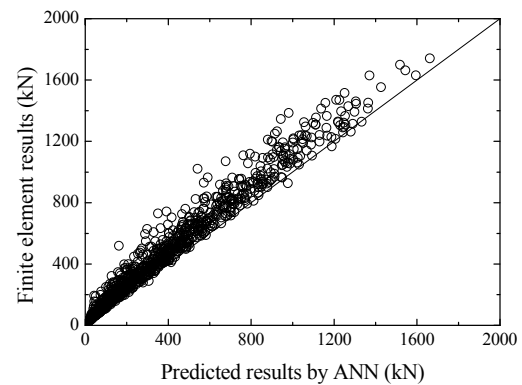


Fig. 9 Comparison predicted results of FEM and ANN for case 3

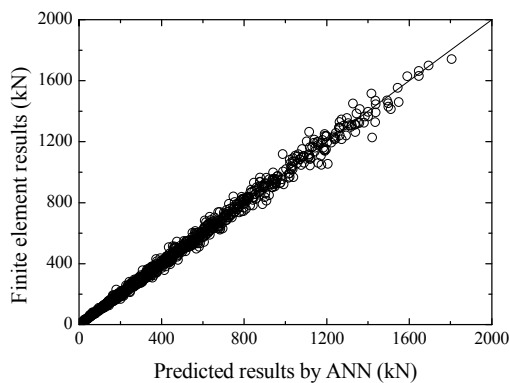


Fig. 7 Comparison predicted results of FEM and ANN for case 1

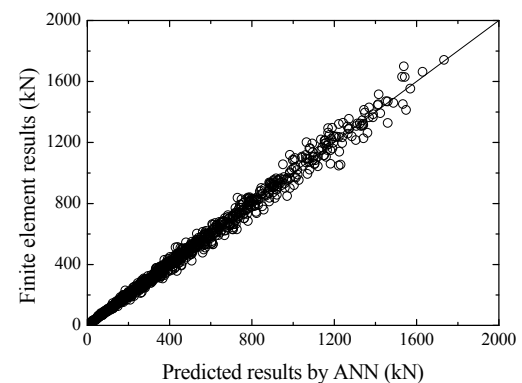


Fig. 10 Comparison predicted results of FEM and ANN for case 4

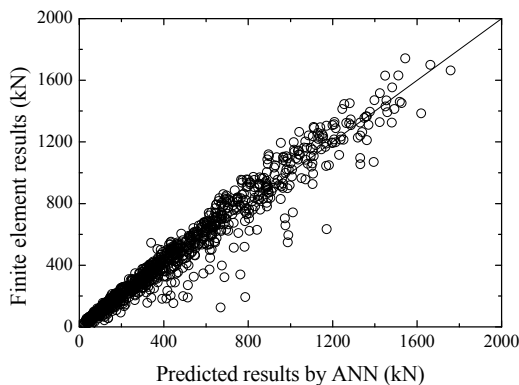


Fig. 8 Comparison predicted results of FEM and ANN for case 2

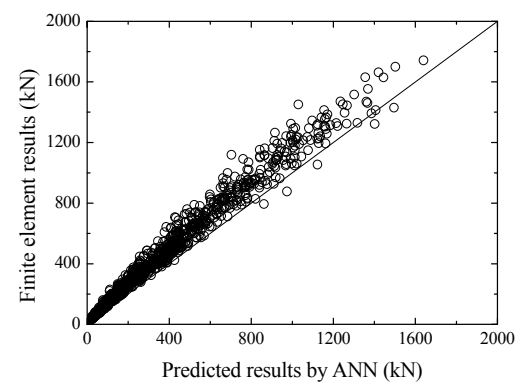


Fig. 11 Comparison predicted results of FEM and ANN for case 5

Table 3 The percentage of mean absolute error percentage for each case

	Mean absolute error percentage %
Case 1	3.7%
Case 2	15.4%
Case 3	23.4%
Case 4	4.6%
Case 5	23.9%

- (3) Parameters in case 2 and standard deviation were included
- (4) Parameters in case 2 and minimum average thickness were included
- (5) Parameters in case 2 and minimum thickness were included

The comparison of predicted results between FEM and ANN for each case show that the error percentage increased significantly when the information on minimum average thickness was taken away from input data, as seen in case 2, case 3 and case 5 stated in Table 3. Since case 1 and case 4 have minimum average thickness data, the error percentages are small. This shows that the information on minimum average thickness is crucial in order to achieve an accurate result. Though the fact that the minimum average thickness is important is already described by other researcher including Appuhamy *et al.* (2011), the present results proves that other parameters also contribute to improve the accuracy, and the accuracy of case 1 and 4 is validated. Note that the case 4 is still meaningful result though the accuracy is not better than the case 1, because the work to measure parameters of case 4 is easier than that of case 1. Therefore, ANN approach now enables us to replace previous approaches such as experimental studies and costly analytical study. Time-consuming and expensive cost problems are solved by the ANN approach.

4.3 Final model

The validity of ANN model was already confirmed in the previous section by LOOCV. In this section, each 1000 data set (input-output) of ten neural network models averaged by the Bagging method in Section 4.1 were

already prepared with a combination of \mathbf{W}_I , \mathbf{b}_I , \mathbf{W}_L and the final output of the ten neural network models can be estimated by using the following Eq. (6).

$$output = \mathbf{W}_L S(\mathbf{W}_I \mathbf{v} + \mathbf{b}_I) + b_L \quad (6)$$

In the above equation, \mathbf{W}_I is the synaptic weight connecting the input layer and hidden layer with the matrix size 8×10 , \mathbf{v} is the input vector with matrix size 10×1 , \mathbf{b}_I is the bias vector which was given to the hidden layer with matrix size 1×8 , S is the sigmoid function expressed in Eq. (2), \mathbf{W}_L is the synaptic weight connecting the hidden layer and the output layer with matrix size 8×1 , b_L is the bias vector which was given to the output layer with matrix size 1×1 .

In this paper, only one matrix output result from the ten ANN model can be given in Fig. 12. The whole matrix size of all ten ANN output results cannot be presented in this paper due to space limitation (in particular \mathbf{W}_I). Therefore, the rest of the networks can be downloaded from the website (http://www.cee.ehime-u.ac.jp/~i_management/supplementdata/ANN_tensile_strength_of_corroded_steel_plates.xlsx) in Microsoft Excel format.

As for Eq. (6), the calculation only employed a simple matrix calculation and exponential functions. Though the computation cost is very low, the proposed neural network model results had good agreement with finite element analysis results. By this simple and inexpensive approach, tensile strength evaluation with high accuracy can be predicted rapidly.

5. Conclusions

In this study, corroded surface data, material properties and FEM results were used to train the ANN model and the accuracy of the model was verified by leave-one-out cross-validation. Initially, in order to verify the FEM, FEM results were compared to experimental results. It was confirmed that the FEM results were accurate. Thereby, the finite element method could then be used to import corroded surface data developed by the spatial autocorrelation model and the artificial corroded models were then analyzed by FEA to obtain tensile strength information. By using the information from corroded surface data, material properties and tensile strength, the ANN model could then be trained.

$$output = \mathbf{W}_L S(\mathbf{W}_I \mathbf{v} + \mathbf{b}_I) + b_L$$

$$\mathbf{W}_I = \begin{bmatrix} -0.048 & 0.005 & 0.001 & 0.000 & -0.002 & 0.007 & -0.059 & 0.103 & -0.016 & -0.164 \\ -0.099 & 0.029 & 0.002 & 0.000 & -0.004 & 0.009 & 0.259 & -0.299 & -0.226 & -0.229 \\ 0.355 & 0.006 & 0.011 & 0.000 & -0.067 & 0.010 & -0.234 & -0.352 & -0.024 & 0.219 \\ 0.092 & 0.003 & 0.000 & 0.000 & -0.001 & 0.013 & -0.096 & -0.063 & 0.031 & 0.068 \\ 0.242 & -0.046 & 0.045 & 0.000 & -0.021 & -0.003 & 0.149 & -0.075 & -0.339 & -0.056 \\ 0.365 & -0.150 & 0.034 & 0.001 & -0.167 & -0.363 & 0.000 & -0.174 & -0.319 & -0.499 \\ -0.275 & -0.207 & -0.018 & 0.001 & -0.499 & -0.068 & -0.319 & -0.322 & -0.318 & -0.067 \\ 0.195 & 0.002 & 0.000 & 0.000 & 0.003 & 0.013 & 0.139 & -0.341 & -1.120 & 0.037 \end{bmatrix}$$

$$\mathbf{b}_I = \{-5.647 \quad 6.346 \quad 11.904 \quad -6.935 \quad -4.979 \quad -0.843 \quad -6.730 \quad -6.568\}^T$$

$$\mathbf{w}_L = \{-2.128 \quad 0.009 \quad -0.008 \quad 0.099 \quad -0.003 \quad -0.005 \quad -0.003 \quad 1.180\}$$

$$b_L = 2.619$$

Fig. 12 Sample of final output of generated network

The ANN results were then compared to FEM results by considering five different cases applied in this study. Cases 2, 3 and 5 have a large mean absolute error percentage due to lack of minimum average thickness information, while cases 1 and 4 have a very small mean absolute error percentage with minimum average thickness information included in the ANN model. This shows that minimum average thickness information is crucial in determining the accuracy of ANN results. It is suggested to always include minimum average thickness information in this proposed approach. With this information, cases 1 and 4 could produce a mean absolute error percentage below 5%. Therefore, in this study, case 1 is selected to confirm the accuracy of the ANN approach. The final output equation in Eq. (6) was also developed for predicting tensile strength in further work where FEM and tensile test are not required to do. Therefore, the ANN approach can be considered as a simple, rapid, and inexpensive method to predict residual tensile strength more accurately.

References

- Ahmmad, M.M. and Sumi, Y. (2010), "Strength and Deformability of corroded steel plates under quasi-static tensile load", *J. Mar. Sci. Technol.*, **15**(1), 1-15.
- Appuhamy, J.M.R.S., Kaita, T., Ohga, M. and Fujii, K. (2011), "Prediction of residual strength of corroded tensile steel plates", *Int. J. Steel Struct.*, **11**(1), 65-79.
- Appuhamy, J.M.R.S., Ohga, M., Kaita, T., Chun, P. and Dissanayake, P.B.R. (2013), "Development of an efficient maintenance strategy for corroded steel bridge infrastructures", *J. Bridge Eng.*, **18**(6), 464-475.
- Bishop, C.M. (2007), *Pattern Recognition and Machine Learning*, Springer, Japan.
- Bozic, D.Z. (1996), "Optimisation of dissolution using artificial neural network", *Farmaceutski Vestnik.*, **47**, 185-186.
- Chun, P. and Inoue, J. (2009), "Numerical studies of the effect of residual imperfection on the mechanical behavior of heat-corrected steel plates, and analysis of a further repair method", *Steel Compos. Struct., Int. J.*, **9**(3), 209-221.
- El-Bakyr, M.Y. (2003), "Feed forward neural networks modeling for K-P interactions", *Chaos Solution. Fract.*, **18**(3), 995-1000.
- Hastie, T., Tibshirani, R. and Friedman, J. (2014), *The Elements of Statistical Learning*, Springer, Japan.
- Hussain, A.S., Yu, X. and Johnson, R.D. (1991), "Application of neural computing in pharmaceutical product development", *Pharm. Res.*, **8**(10), 1248-1252.
- Hussain, A.S., Shivanand, P. and Johnson, R.D. (1994), "Application of neural computing in pharmaceutical product development", *Comput. Aid. Formul. Des., Drug Development and Industrial Pharmacy*, **20**(10), 1739-1752.
- Kaita, T., Tagaya, K., Fujii, K., Miyashita, M. and Uenoya, M. (2005), "A simple estimation method of bending strength for corroded plate girder", *Collab. Harmoniz. Creative Syst.*, **1**, 89-97.
- Kaita, T., Appuhamy, J.M.R.S., Ohga, M. and Fujii, K. (2012), "An enhanced method of predicting effective thickness of corroded steel plates", *Steel Compos. Struct., Int. J.*, **12**(5), 379-393.
- Khedmati, M.R., Nouri, Z.H.M.E. and Roshanali, M.M. (2011), "An effective proposal for strength evaluation of steel plates randomly corroded on both sides under uniaxial compression", *Steel Compos. Struct., Int. J.*, **11**(3), 183-205.
- Muranaka, A., Minata, O. and Fujii, K. (1998), "Estimation of residual strength and surface irregularity of the corroded steel plates", *J. Struct. Eng.*, **44A**, 1063-1071. [In Japanese]
- Murtoniemi, E., Merkkü, P. and Yliruusi, J. (1993), "Comparison of four different Neural network training algorithms in modelling the fluidized bed granulation process", *Lab. Microcomp.*, **12**(3), 69-76.
- Ohga, M., Appuhamy, J.M.R.S., Kaita, T., Chun, P. and Dissanayake, P.B.R. (2011), "Degradation of tensile strength with the severity of corrosion condition", *Proceedings of World Congress on Advances in Structural Engineering and Mechanics (ASEM11+)*, Seoul, Korea, September, pp. 5280-5297.
- Okumura, M., Fujii, K. and Tukai, M. (2001), "Statistical model of steel corrosion considering spatial auto-correlation", *J. JSCE*, **672**, 109-116. [In Japanese]
- Rahgozar, R., Sharifi, Y. and Malekinejad, M. (2010), "Buckling capacity of uniformly corroded steel members in terms of exposure time", *Steel Compos. Struct., Int. J.*, **10**(6), 475-487.
- Richardson, C.J. and Barlow, D.J. (1996), "Neural network computer simulation of aerosols", *J. Pharm. Pharmacol.*, **48**(6), 581-591.
- Sugimoto, I., Kobayashi, Y. and Ichikawa, A. (2006), "Durability evaluation based on buckling characteristics of corroded steel deck girders", *Quarterly Rep. of Railway Technical Research Inst. (QR of RTRI)*, **47**(3), 150-155.
- Zhang, G.P. (2003), "Time series forecasting using a hybrid ARIMA and neural network model", *Neurocomputing*, **50**, 159-175.

CC